Borocarbide Precipitation in the HAZ of Boron Steel Welds

The amount of intergranular borocarbides occurring in the HAZ of boron steel during weld cooling was found to be dependent upon weld cooling rate and the peak HAZ temperature

BY J. H. DEVLETIAN

ABSTRACT. When boron steels are welded, the HAZ of these welds are susceptible to borocarbide precipitation at prior austenite grain boundaries. The literature establishes that extensive intergranular precipitation can significantly decrease not only boron's hardenability effect but also the steel's notched toughness. Consequently, the objective of this study was to determine and evaluate the primary factors controlling the formation of intergranular borocarbides in the HAZ.

In this work, single-pass manual SMA and automatic GMA welds were deposited on 10B20 boron steel plate. An extremely wide range of cooling rates from 0.02 to 160 F/s at 1300 F were studied.

The prime factor controlling the amount of intergranular borocarbide precipitation occurring in the HAZ of 10B20 steel was found to be weld cooling rate. There was an optimum weld cooling rate of 3.7 F/s which produced a maximum amount of intergranular borocarbides; while, for extremely fast cooling rates of 140 F/s or greater, no intergranular precipitation occurred. However, at extremely slow cooling rates as low as 0.02 F/s, the amount of intergranular borocarbide particles diminished substantially but the average particle size increased. Furthermore, it was found that the higher the peak temperature in the HAZ, the greater the tendency to form intergranular borocarbides upon cooling. In all cases, extensive intergranular borocarbide precipitation could be completely eliminated by postweld annealing or normalizing between 1580 and 1700 F. Although welds were deposited by both the SMAW and GMAW processes, the welding process used was not a factor in the formation of borocarbides in the HAZ.

J. H. DEVLETIAN is Assistant Professor, Materials Science, Department of Chemical Engineering and Materials Science, Youngstown State University, Youngstown, Ohio 44555.

Introduction

Boron, in amounts from 0.001 to 0.003%, can be added to steel to increase hardenability; and, so long as the boron remains in solid solution, boron's effectiveness is fully utilized. However, under certain conditions, extensive borocarbide precipitation may occur at austenite grain boundaries thereby greatly impairing the steel's hardenability and notch toughness. This investigation evaluates boron's borocarbide-forming tendencies in the HAZ of 10B20 boron steel welds, as-deposited by the SMA (shielded metal-arc) and GMA (gas metal-arc) welding processes.

Although little is known about the behavior of boron in the HAZ of steel welds, much insight can be gained by briefly reviewing some of the factors which promote intergranular borocarbide formation in wrought steels and steel weld metal. In their study of ASTM A514-type J wrought steel, Melloy et al (Ref. 1) found that there was an optimum boron content of 0.0020% corresponding to maximum hardenability and best notch toughness. A progressive loss of toughness with increasing boron content beyond 0.0025% was attributed to the formation of borocarbide particles of composition $Fe_{23}(B,C)_6$ at prior austenite grain boundaries. The amount of intergranular borocarbide precipitation was not only a function of boron content but also of austenitizing temperature. Grange and Mitchell (Ref. 2) proved that the loss in hardenability when 86Bxx type boron steels were austenitized at excessively high temperatures was directly related to the kinetics of precipitation of these borocarbides. The higher the austenitizing temperature, the greater the propensity to form intergranular borocarbides during subsequent cooling to a lower temperature and the greater the loss of boron's hardenability effect in the steel.

Similarly, in recent work on 10B20 boron steel weld metal, Heine and Devletian (Ref. 3) have shown that under certain conditions borocarbides readily precipitated at prior austenite grain and cell boundaries; and, that the amount of precipitation was dependent upon weld cooling rate as well as the initial boron content of the weld. Furthermore, there was also an optimum boron content of approximately 0.002% corresponding to maximum hardenability and notched tensile strength. Any loss of these weld metal properties was directly attributed to the formation of excessive amounts of intergranular borocarbides during weld cooling.

Based on the preceding information, the HAZ of a weld deposited on boron steel plate should be particularly susceptible to such detrimental borocarbide precipitation at prior austenite grain boundaries due to the extremely high peak temperatures experienced during welding. Although the time duration of a typical heating and cooling cycle in the HAZ is quite short, the peak temperatures can be as high as the incipient melting temperature at the weld-base metal interface or as low as the eutec-

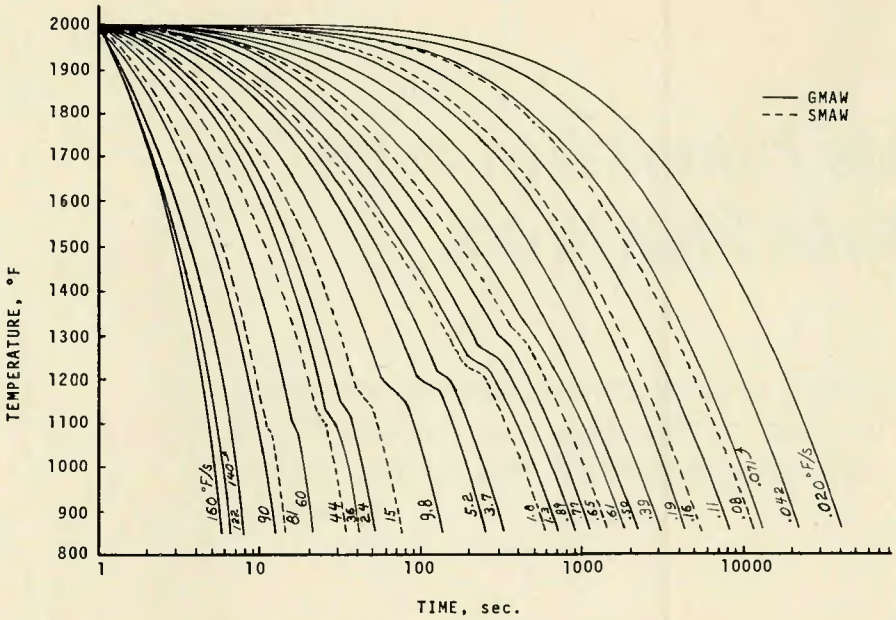

Fig. 1 — Cooling curves of weld metal deposited by the GMAW and SMAW processes on 10B20 boron steel. The 1300 F weld cooling rate is indicated on each curve

toid transformation temperature at the outer edges of the HAZ. Thus, the formation of intergranular borocarbides in the HAZ of a boron steel should be contingent not only upon the weld cooling rate but also upon the peak temperature.

Consequently, the objectives of this investigation were (a) to establish the effect of weld cooling rate and other time-temperature parameters upon the amount of borocarbide precipitation occurring in the HAZ of commercial 10B20 boron steel, (b) to determine the factors contributing to the formation or dissolution of borocarbides and (c) to predict by a simple mathematical model the amount of intergranular borocarbides which will form in the HAZ of SMA and GMA welds.

Procedure

Materials

This study was performed on commercially available 10B20 boron steel plate containing: 0.0017% B, 0.19% C, 0.76% Mn, 0.22% Si, 0.08% Al, 0.011% P and 0.022% S. Specimen thicknesses of 1/8, 1/4, 3/8 and 1/2 in. were fabricated by cold rolling. These specimens were then cut into 10 in. long by 8 in. wide sections and were annealed at 1600 F in an argon atmosphere.

Welding

All welding was performed by the automatic gas metal-arc welding (GMAW) and the manual shielded metal-arc welding (SMAW) processes. Single pass bead-on-plate welds were deposited on 10B20 steel specimens containing a U-groove. Filler metals used in the GMAW process were 0.045 in. and 0.094 in. diam E70S-2 wire. Argon shielding gas (35 cfh) was used to protect the GMA welds. In the manual SMAW process, E7018 covered electrodes were used to weld the boron steel specimens.

Cooling Rate Determination

Temperature measurement of the weld metal during solidification and subsequent cooling was accomplished by plunging an 0.020 in. diam W-3% Re/W-25% Re thermocouple directly into the molten weld pool behind the moving arc. The entire cooling curve for each weld was recorded automatically on a continuous chart recorder.

To determine the weld cooling rate at 1300 F, a line was drawn tangent to the cooling curve at 1300 F. Since the plot of millivolts vs. temperature for this W-3% Re/W-25% Re thermocouple was linear in the range of 500 F to 2800 F, weld cooling rates at 1300 F were calculated directly from the chart recordings for maximum accuracy.

Controlling Weld Cooling Rate

The weld and HAZ cooling rates were controlled by judicious selection of welding variables. Fast cooling rates, greater than 80 F/sec. for example, were obtained by welding the 1/2 in. thick plates with low arc energy input, no preheating and efficient metal-to-metal heat transfer from the workpiece to a cold copper backing plate.

Conversely, slow cooling rates were obtained by welding the thinnest specimens (1/8 in. thick) with high heat input, preheating in an atmosphere controlled furnace to as high as 1000 F and using a similarly preheated steel backing plate. In order to obtain extremely slow weld cooling rates, i.e., less than 0.40 F/sec, special 1/4 × 2 × 2 in. preheated specimens were welded with maximum possible heat input for this thickness and then immediately (while the weld temperature was still above 2200 F) inserted into a furnace previously preheated to as high as 2000 F and furnace cooled in an argon atmosphere to prevent deboronization. This procedure permitted the study of borocarbide precipitation in the HAZ far beyond the widest possible range of weld cooling rates encountered in commercial GMA and SMA welding operations.

Determination of Peak Temperatures in the HAZ

In order to evaluate the effect of peak temperatures on the amount of borocarbide precipitation occurring in the HAZ, the entire range of HAZ peak temperatures from the weld fusion line to the outer periphery of the HAZ had to be determined. For maximum accuracy, this was accomplished by combining actual peak temperature data from thermocouples embedded in the HAZ with the Adams equation (Ref. 5). The Adams equation states:

$$\frac{1}{T_p - T_o} = \frac{4.133\rho C_p dtV}{q} + \frac{1}{T_m - T_o}$$

T_p = peak temperature, F, at distance, d, from fusion line
T_o = initial plate temperature, F
T_m = plate melting temperature, F
ρ = density, lb/ft^3
C_p = specific heat, Btu/lb-F
d = distance from weld fusion boundary, ft
q = rate of heat flow from arc, Btu/h
V = arc travel speed, ft/h
t = plate thickness, ft

However, in this equation ρ and C_p were not constant but varied with temperature. Furthermore, T_p also varied with different methods of heat removal from the weld such as using high conductivity vs. low conductivity backing plates. Thus, experimental values of $4.133\rho C_p tV/q$ had to be determined for each weld for maximum accuracy.

To do this, welds were deposited on 10B20 steel containing several W-3% Re/W-25% Re thermocouples at various distances from the fusion line. The thermocouple bulbs were ground to 0.010 in. diam and welded into the 10B20 steel surface at various distances from the U-groove. Upon

depositing the weld metal into the U-groove, the peak HAZ temperature at the thermocouple location was recorded. The exact distance between the fusion line and the center of the thermocouple was determined by making a transverse-to-weld metallographic section and measuring this distance under the microscope. Once a particular peak temperature and its corresponding distance from the weld were experimentally determined, a value for $4.133\rho C_p tV/q$ could be calculated for the 10B20 steel workpiece.

For example, a thermocouple had been embedded just outside the area to be welded. After welding, d was measured to be 0.0141 ft and T_p was 1300 F. Letting $G = 4.133\rho C_p tV/q$ and solving for the quantity represented by G, the Adams equation yielded:

$$G = \left[\frac{1}{T_p - T_0} - \frac{1}{T_m - T_0}\right]\frac{1}{d}$$

$$= \left[\frac{1}{1300-80} - \frac{1}{2723-80}\right]\frac{1}{0.0141}$$

$$G = 0.03133/\text{F-ft}$$

This procedure was repeated several times for this particular set of welding parameters and the value of 0.03133/F-ft was found to be quite consistent.

Using an average value of G = 0.03133, the Adams equation reduced to:

$$\frac{1}{T_p - 80} = 0.03133\ d + \frac{1}{2723 - 80}$$

Now the peak temperature in the HAZ could be plotted as a function of distance, d. However, the value of the constant G had to be redetermined whenever the plate thickness and/or welding parameters were changed.

Metallography

All metallography of the HAZ structures was performed on transverse-to-weld sections in the immediate area of the embedded thermocouple for the most accurate correlation between weld cooling rate and HAZ microstructure. These sections were electrolytically polished with a CrO_3 solution and then etched in picral.

Results and Discussion

Weld Cooling Curves

During the welding of 10B20 boron steel specimens by the GMAW and SMAW processes, cooling curves were recorded for each weld. In Fig. 1, several typical SMAW and GMAW cooling curves are presented to illustrate the great range of weld cooling rates which were investigated. The abscissa of Fig. 1 had to be plotted logarithmically due to the large differences in cooling times between the fastest and the slowest cooling welds. Since the cooling curves around 1300 F were of great interest in the work, the starting point on the chart recorder for each curve was arbitrarily set at 2000 F and finishing temperature was set at 800 F, below which readings were no longer taken. Cooling curves representing weld cooling rates between 2 to 80 F/s measured at 1300 F are typical of SMAW and GMAW cooling rates encountered in commercial welding applications. Specimens with weld cooling rates less than 0.4 F/s or greater than 80 F/s were also studied in order to examine the borocarbide precipitation phenomenon in the HAZ over the widest possible range of weld cooling rates practicable.

From Fig. 1, it is strikingly clear that the welding process had no appreciable effect upon the shape of the cooling curves. Welds deposited on 10B20 steel by either the manual SMAW or GMAW processes exhibited similar weld cooling curves provided the weld cooling rate at 1300 F was the same. This strongly suggested that any metallurgical phenomena occurring in the HAZ of SMA and GMA welds would be primarily a function of weld cooling rate and not the welding process.

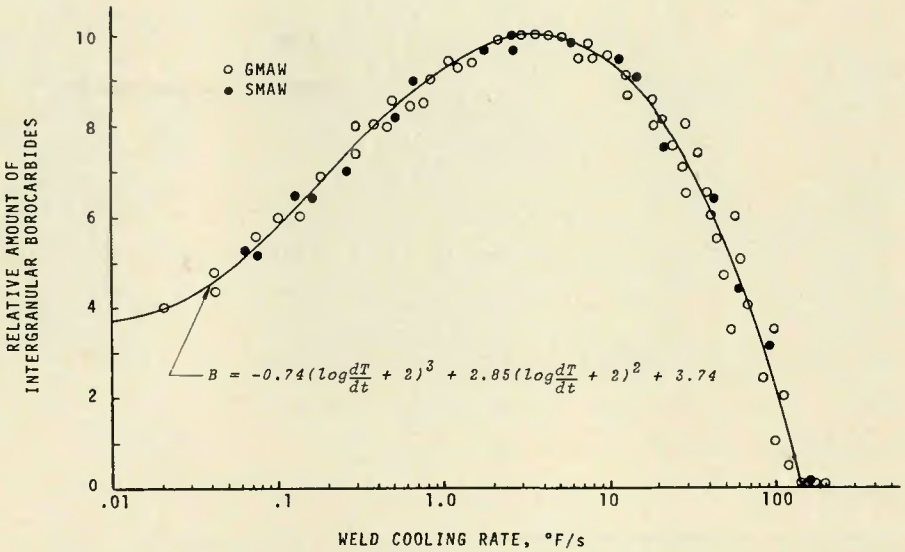

Fig. 2 — Effect of 1300 F weld cooling rate on the amount of intergranular borocarbides precipitating in the HAZ of 10B20 steel

Soluble vs. Insoluble Boron

In the commercial 10B20 steel used in this study, the total boron concentration was 0.0017% of which 0.0009% was chemically analyzed to be "soluble" or uncombined boron while 0.0008% was "insoluble" or combined boron. Only the soluble boron was of interest in this investigation because it was this soluble interstitial boron which was responsible for the formation of intergranular $Fe_{23}(B,C)_6$ borocarbides in the HAZ of boron steel.

The combined boron, on the other hand, is known to have no significant effect upon either mechanical properties or hardenability of commercial boron steels. In the HAZ microstructure of 10B20 steel, combined boron appeared as widely scattered particles of boron-containing compounds which did not dissolve nor did they partake significantly in any metallurgical reactions during normal thermal processing. Thus, only interstitial boron was of importance in this investigation, and any reference hereafter to the word "borocarbides" refers to $Fe_{23}(B,C)_6$ which is formed from interstitial boron at austenite grain boundaries.

Occurrence of Borocarbides in HAZ

The amount of borocarbides forming at the prior austenite grain boundaries in the HAZ of 10B20 steel welds was found to be a function of the weld cooling rate as shown in Fig. 2. Whether the welds were deposited by the SMAW or GMAW processes made no apparent difference. Only the cooling rate controlled the amount of intergranular borocarbides occurring in the HAZ of SMA and GMA welds.

For extremely fast weld cooling rates of 140 F/s or greater, no appreciable quantities of intergranular borocarbides precipitated in the HAZ, as shown in Fig. 2. However, as the weld cooling rate decreased from 140 F/s to 3.7 F/s, the amount of intergranular borocarbides increased up to a maximum amount. With further decreases in weld cooling rate from 3.7 F/s to 0.02 F/s, the number of intergranular borocarbide particles

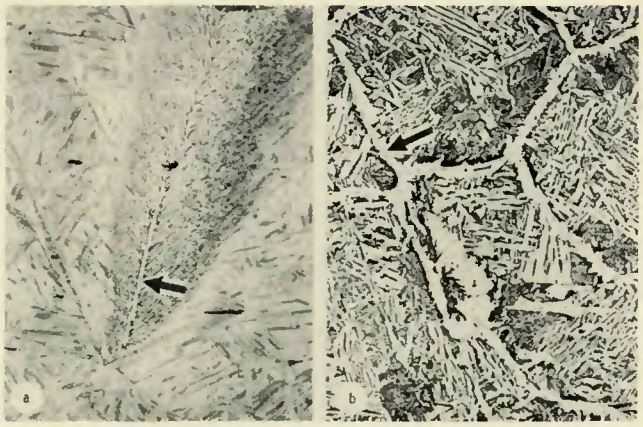

Fig. 3 — HAZ microstructures of 10B20 steel for weld cooling rates of (a) 90 F/s and (b) 39 F/s. Arrows point to intergranular borocarbide particles. Etchant: picral. X600, reduced 52%

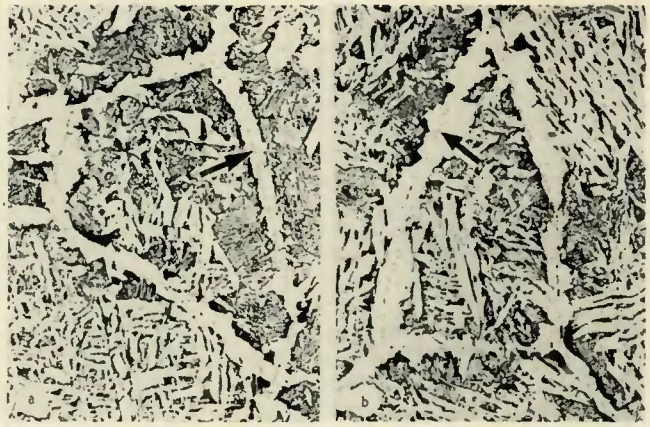

Fig. 4 — HAZ microstructures of 10B20 steel for weld cooling rates of (a) 21 F/s and (b) 11 F/s. Etchant: picral. X600, reduced 52%

Table 1 — Criteria Used for Rating the Relative Amount of Borocarbides at Prior Austenite Grain Boundaries in the HAZ of 10B20 Steel

Rating	Explanation
0	No borocarbides at boundaries.
2	Short stringers[a] along a few boundaries.
4	Short and long stringers[a] in about half all boundaries.
6	Long stringers[a] in about two-thirds all boundaries.
8	Long stringers[a] in most boundaries.
10[b]	Long stringers[a] in essentially all boundaries.

(a) "Stringer" is defined here as a row of unconnected borocarbide particles distributed along a prior austenite grain boundary.
(b) The rating of 10 represents the maximum amount of precipitation observed in any HAZ of 10B20 steel.

gradually decreased while the average particle size tended to become coarser.

The equation which best fits the data presented in Fig. 2 obeys the relationship:

$$B = -M(\log \frac{dT}{dt} + L)^3 + J(\log \frac{dT}{dt} + L)^2 + K \qquad (1)$$

where dT/dt is the weld cooling rate measured at 1300 F and B is the relative amount of borocarbide particles precipitating at prior austenite grain boundaries in the HAZ. The amount of intergranular borocarbides, B, can vary from the arbitrarily set limits of zero (no appreciable amount of intergranular borocarbides) to a maximum of 10 (maximum quantity of intergranular borocarbides) according to Table 1. The criteria set forth in Table 1 for measuring relative quantities of borocarbides had to be devised due to the extreme difficulty in measuring the absolute quantity of intergranular borocarbide particles in the HAZ microstructure. The values of the constants K, J, L and M in equation 1 were evaluated to fit the data in Fig. 2. The values of these constants are dependent primarily upon the boron and alloy content of the particular steel.

Hence, in this investigation, the amount of borocarbides precipitating in the HAZ of 10B20 steel during weld cooling was determined to be:

$$B = -0.74(\log \frac{dT}{dt} + 2)^3 + 2.85(\log \frac{dT}{dt} + 2)^2 + 3.74 \qquad (2)$$

This equation can also be expressed in its equivalent form:

$$B = -0.74(\log \frac{dT}{dt})^3 - 1.59(\log \frac{dT}{dt})^2 + 2.52 \log \frac{dT}{dt} + 9.22 \qquad (3)$$

Equations 2 and 3 are the "best fit" equations for the experimental data shown in Fig. 2 and therefore apply specifically to SMA and GMA welds deposited on 10B20 steel provided the 1300 F weld cooling rate is within the range:

$$0.02 \text{ F/s} < dT/dt < 140 \text{ F/s}$$

Detection of Borocarbides in HAZ

Optical metallographic techniques proved to be the only simple yet effective method of clearly observing the presence of $Fe_{23}(B,C)_6$ borocarbides at prior austenite grain boundaries in the HAZ of 10B20 steel welds. Other techniques such as electron microprobe analysis and neutron-activated autoradiography by the method of Hughes and Rogers (Ref. 4) were tried but shown to be ineffectual. The electron microprobe was unable to detect the low boron content used in boron steel and activated boron metallography required painstaking labor to obtain somewhat limited information for the intended purpose of this investigation.

10B20 boron steel was ideally suited for metallographic analysis because its hardenability was low enough that, upon weld cooling, white-etching proeutectoid ferrite completely enveloped the prior austenite grain boundaries even up to weld cooling rates as fast as 90 F/s. This greatly facilitated the detection of borocarbides at prior austenite grain boundaries since the dark-etching borocarbide precipitates were clearly delineated against a "white" background of blockly or proeutectoid ferrite as illustrated, for example, by the microstructures in Figs. 3 through 7.

For weld cooling rates faster than 90 F/s, the task of observing the presence of intergranular borocarbides in a martensitic matrix was still practicable. Since martensite etched much lighter than $Fe_{23}(B,C)_6$, the intergranular borocarbides were easily exposed. Thus, borocarbides in the HAZ of 10B20 steel were accurately observed throughout the extremely wide range of weld cooling rates studied.

Microstructures of HAZ vs. Cooling Rate

The effect of GMA weld cooling rate upon the amount of intergranular borocarbide precipitation and upon other structural features in the HAZ of 10B20 steel is illustrated by the microstructures in Figs. 3 through 7. For ease of comparison, these microstructures were all photographed at X600 and arrows were superimposed on each photomicrograph to point out the borocarbides which have precipitated at prior austenite grain boundaries. Furthermore, it was found that the HAZ microstructures of SMA welds were virtually identical to those of GMA welds. Thus, to avoid repetition, only the HAZ microstructures of GMA welds were presented in Figs. 3 through 7.

When GMA welds, deposited on 10B20 steel were cooled at weld cool-

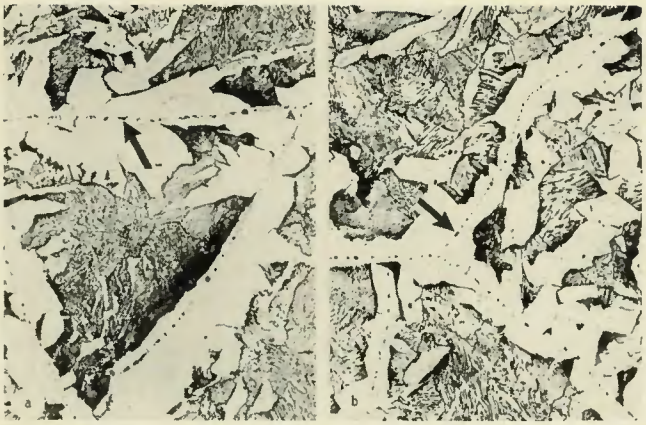

Fig. 5 — HAZ microstructures of 10B20 steel for weld cooling rates of (a) 3.7 F/s and (b) 3.0 F/s. Etchant: picral. X600, reduced 52%

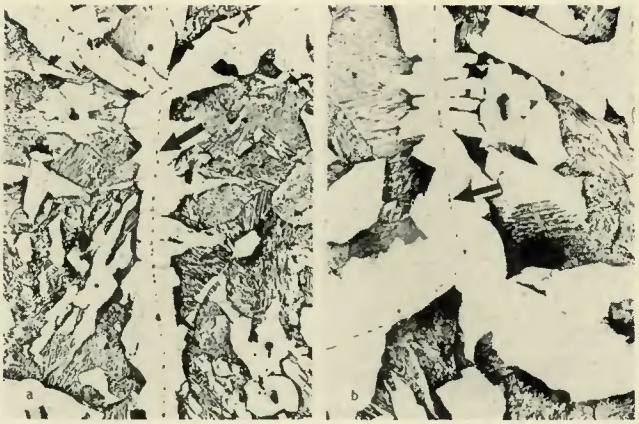

Fig. 6 — HAZ microstructures of 10B20 steel for weld cooling rates of (a) 2.2 F/s and (b) 0.89 F/s. Etchant: picral. X600, reduced 52%

ing rates greater than 140 F/s, only negligible quantities of intergranular borocarbide precipitation occurred in the HAZ (Fig. 2). The microstructures of these rapidly cooled HAZ's were entirely martensitic. However, as the weld cooling rate was decreased to 140 F/s, the first traces of distinct borocarbide precipitation at prior austenite grain boundaries appeared. Again, because of the rapid weld cooling rate, the matrix of this HAZ was entirely martensitic.

At 90 F/s, more intergranular borocarbides precipitated in the HAZ as shown in Fig. 3a. Here, the borocarbides consisted of a few very fine particles along the prior austenite grain boundaries from which upper bainite had also precipitated. This microstructure contained nearly all martensite with some small regions of upper bainite. The amount of intergranular borocarbides in the HAZ corresponded to a rating of 2.5 (see Table 1) out of a maximum of 10.

As the weld cooling rate was further decreased below 90 F/s, the amount of borocarbides forming at prior austenite grain boundaries continued to increase until a maximum amount of precipitation occurred at the optimum cooling rate of 3.7 F/s. Figures 3b, 4a, 4b and 5a represent weld cooling rates of 39, 21, 11 and 3.7 F/s respectively.

At a weld cooling rate of 39 F/s, the amount of intergranular borocarbides corresponded to a rating of 6 (see Fig. 2); while, at the optimum cooling rate of 3.7 F/s, the amount of borocarbides corresponded to a maximum rating of 10. However, as the amount of intergranular precipitation increased with decreasing cooling rate, the average borocarbide particle size increased slightly. The structure of the HAZ gradually changed from bainitic at 39 F/s to a mixture of bainite and fine pearlite at 3.7 F/s, while, the amount of proeutectoid ferrite increased correspondingly with decreasing cooling rate.

Upon decreasing the weld cooling rate from the optimum rate of 3.7 F/s down to an extremely slow rate of 0.02 F/s, the following microstructural changes occurred as observed in Figs. 5, 6 and 7: (a) the amount of intergranular borocarbides decreased from a maximum rating of 10 at 3.7 F/s to 4 at 0.02 F/s (Fig. 2), (b) on the average, each borocarbide particle became coarser, (c) the amount of proeutectoid ferrite increased and (d) the lamellar spacing of pearlite increased.

Thus, in this microstructural study of the HAZ of 10B20 boron steel, the amount of intergranular borocarbide precipitation was indeed found to be dependent upon the weld cooling rate in the manner described by equation 2 and Fig. 2. Furthermore, the average borocarbide particle size at prior austenite grain boundaries was also found to be dependent upon cooling rate.

Predicting the Presence of Borocarbides in HAZ

Since the precipitation of borocarbides was completely dependent upon weld cooling rate, it now becomes possible to predict the quantity of intergranular borocarbides occurring in the HAZ before the weld is even made. This can be done simply by calculating the anticipated weld cooling rate at 1300 F and substituting this value into equation 2. For example, suppose a certain thickness of 10B20 boron steel plate is going to be welded by either the GMAW or SMAW processes using an arc energy input of 6000 joules/in. The weld cooling rate at 1300 F can be readily calculated by applying the methods of Signes (Ref. 6), Dorschu (Ref. 7) or others. Using Signes equation, the 1300 F weld cooling rate for 2-dimensional heat flow in SMA and GMA welds can be calculated as follows:

$$\frac{dT}{dt} = B_1 \frac{p^2 (1300 - T_0)^3}{E^2} \qquad (4)$$

p = plate thickness
E = heat input measured at welding head
T_0 = initial temperature of plate
B_1 = experimental constant

Once the cooling rate has been calculated (and suppose the cooling was hypothetically calculated to be 3 F/s) substitution of this value into equation 2 yields:

$$B = -0.74 (\log 3 + 2)^3 + 2.85 (\log 3 + 2)^2 + 3.74$$
$$B = 9.9$$

The amount of borocarbides occurring in 10B20 HAZ is 9.9 out of a maximum possible rating of 10. This would be comparable to the microstructure shown in Fig. 5b. Such a large amount of intergranular borocarbide precipitation could possibly decrease not only the notched toughness as indicated by Melloy et al (Ref. 1) but also boron's hardenability effect in the HAZ.

Peak HAZ Temperature va. Borocarbide Formation

In the previous sections, it has been established that intergranular borocarbide precipitation in the HAZ was dependent upon weld cooling rate as shown in Fig. 2. This is quite true, but, the distribution of intergranular borocarbides throughout the entire HAZ of 10B20 boron steel was not found to be perfectly uniform. In fact, only about one-third of the HAZ actually contained fully developed borocarbides while the rest of the HAZ contained little or no precipitation as illustrated in Fig. 8a. Although Fig. 8a

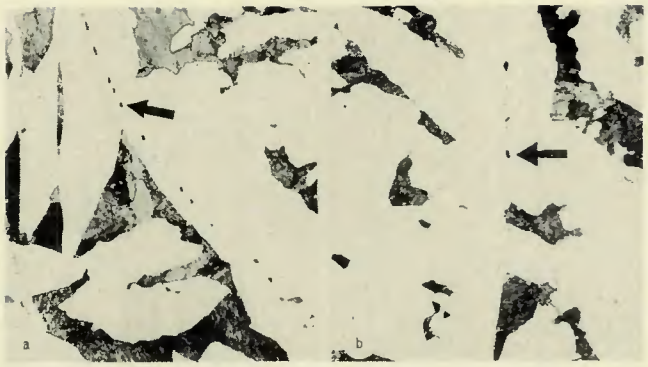

Fig. 7 — HAZ microstructures of 10B20 steel for weld cooling rates of (a) 0.19 F/s and (b) 0.02 F/s. Etchant: picral. X600, reduced 52%

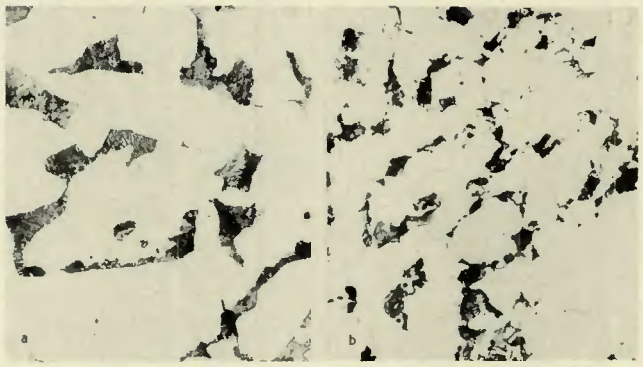

Fig. 9 — Microstructures of the HAZ of 10B20 steel after postweld (a) annealing and (b) normalizing at 1650 F — 1 h. Figure 5(a) shows this HAZ microstructure before heat treating. Etchant: picral. X600, reduced 52%

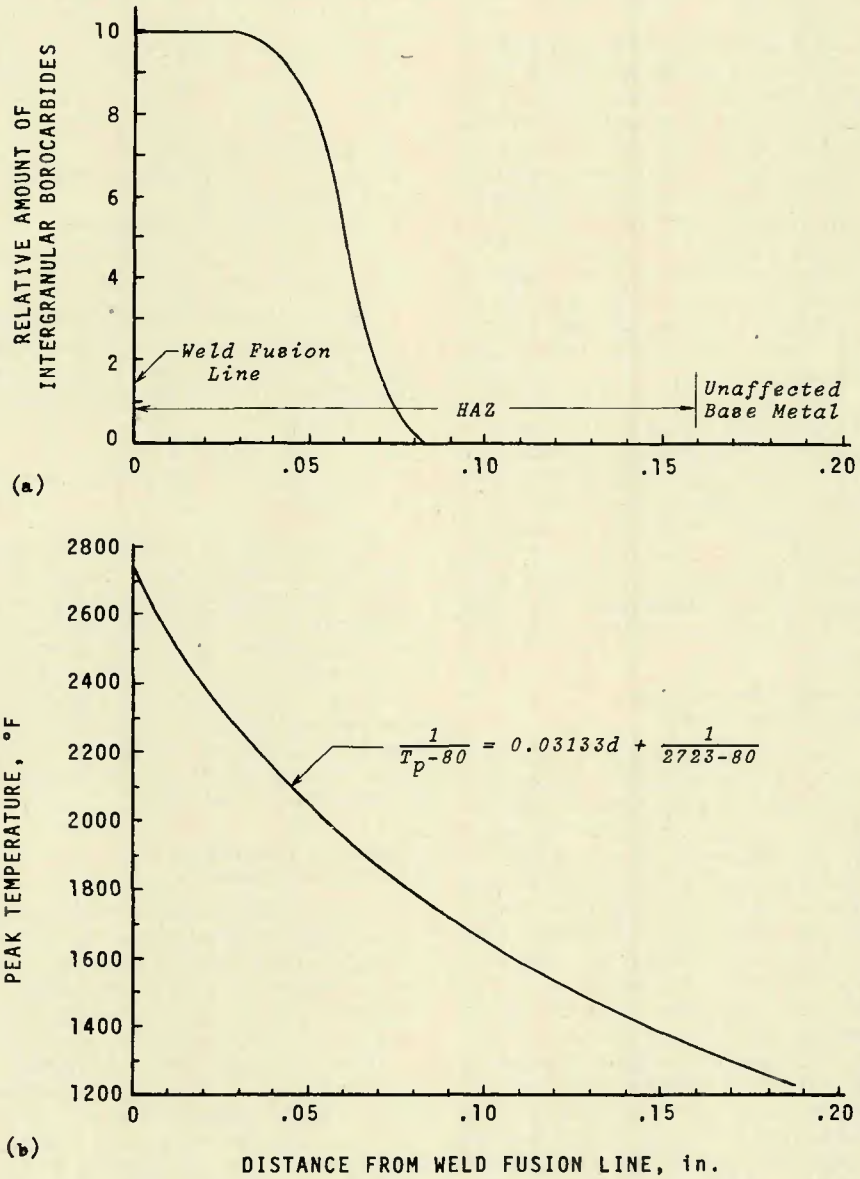

Fig. 8 — Relationship between (a) the density distribution of intergranular borocarbides within the HAZ of 10B20 steel and (b) the peak HAZ temperatures as a function of distance from the weld fusion line. Welded by GMAW process and cooled at 3.0 F/s

represents only one particular welded specimen, it is typical of the borocarbide distribution which occurs in the HAZ of 10B20 steel.

This behavior of boron strongly indicates that the distribution of borocarbides in the HAZ is dependent not only upon cooling rate but also upon the peak temperature. From Fig. 8a and b, it can be seen that any peak temperature in the HAZ greater than approximately 2100 F produced intergranular borocarbides in the amounts indicated in Fig. 2 for a particular weld cooling rate. Clearly, those parts of the HAZ which were close to the weld fusion line experienced high peak temperatures (i.e., high into the austenite range) and therefore exhibited substantial precipitation upon cooling. However, the actual amount of borocarbide precipitation was dependent upon weld cooling rate. Peak temperatures in the HAZ of less than approximately 1750 F resulted in no appreciable borocarbide precipitation at austenite grain boundaries. These findings generally concur in principle with those of Grange and Mitchell (Ref. 2) in that high austenitizing temperatures in boron steel produce intergranular borocarbides while low austenitizing temperatures do not.

Elimination of Borocarbides by Heat Treatment

Postweld annealing or normalizing was found to be an excellent method to effectively eliminate all traces of intergranular borocarbides from the HAZ of 10B20 boron steel. Borocarbides were efficiently removed by normalizing or annealing within the temperature range of 1580 to 1700 F. For example, the welded specimen whose HAZ contained large amounts of intergranular borocarbides (shown in Fig. 5a) was subsequently annealed at 1650 F for one hour. The resulting microstructure shown in Fig. 9a proved that the HAZ after having been annealed contained no observ-

able intergranular borocarbides. Postweld normalizing produced similar results as shown in Fig. 9b. However, annealing or normalizing temperatures significantly higher than 1700 F (especially above 2000 F) resulted in renewed borocarbide precipitation at the austenite grain boundaries.

Heat treatments which interrupted the weld cooling process also affected the amount of intergranular borocarbide precipitation in HAZ. It was found that borocarbides could be greatly reduced in the HAZ of SMA and GMA welds if the weld were extremely slowly cooled through the temperature range from 1750 F to 1580 F to allow maximum time for agglomeration of borocarbides. As an illustration, a weld was made using welding parameters necessary to insure a weld cooling rate of 3 to 4 F/s at 1300 F. However, before the weld could cool below 2200 F, the weld (and attached thermocouple) was quickly inserted into an adjoining furnace preheated to 1650 F. The specimen was held in the furnace at 1650 F for one-half hour and then air-cooled. The resulting microstructure exhibited a substantial reduction in the total number of intergranular borocarbides but the average size of each particle was noticeably coarser. The actual amount of intergranular borocarbides in this HAZ corresponded to a rating of 5; while, of course, if this same weld were permitted to cool normally, without holding at 1650 F in a furnace, it would have precipitated a maximum amount of borocarbides corresponding to a rating of 10 similar to those HAZ structures shown in Fig. 5.

Explanation of Boron's Behavior in HAZ

Although much has been reported concerning the mechanism of boron's behavior in wrought steels, little is actually fully understood. In this study, it was found that the precipitation of intergranular borocarbides in the HAZ of 10B20 boron steel was dependent upon weld cooling rate in a manner illustrated in Fig. 2. Such precipitation during weld cooling was in fact quite difficult to avoid. Yet, when the weld cooling rate was extremely fast (140 F/s) or when a postweld normalizing heat treatment was performed, the intergranular borocarbides vanished from the HAZ of GMA or SMA welds.

Such behavior suggests that boron, which is an oversized interstitial atom in austenite, has a strong tendency to form solute atmospheres in and around grain boundaries as well as dislocations. Since the strain energy of an average high-angle grain boundary is significantly greater than that of a dislocation and since the dislocation density in fully recrystallized austenite is only minimal, substantially more boron would be expected to concentrate at austenite grain boundaries than at dislocations. Thus, the formation of an atmosphere in and around a boundary would lower the elastic strain energy of not only the boundary but also that associated with each interstitial boron atom.

In the HAZ of welds, where heating to peak temperatures and subsequent cooling occur quickly, diffusion of boron to grain boundaries must also occur rapidly in order to account for the large amount of intergranular borocarbides precipitating at cooling rates below 140 F/s. Furthermore, at peak temperatures above 2100 F, the growth rate of austenite grains is substantial; and, as the grain boundaries sweep out across large volumes of metal during the grain growth phase of this thermal cycle, a large percentage of boron atoms come into contact with boundaries of austenite grains. Since the boundary represents an "energy well" for interstitial atoms, many boron atoms remain in and around the boundary. During subsequent cooling, however, the solid solubility of boron in 0.20% carbon steel decreases with decreasing temperature so that the boundaries of austenite become supersaturated. With additional cooling through the lower regions of the austenite field, the grain boundaries become so supersaturated that intergranular borocarbide precipitation results. The degree of precipitation is greatly dependent upon both the weld cooling rate and the peak austenitizing temperatures experienced by the HAZ.

The weld cooling rate is a controlling factor over the precipitation of borocarbides because the processes of nucleation and growth are time-dependent phenomena. As the weld cooling rate is increased from the optimum value of 3.7 F/s to 140 F/s, the concentration of intergranular borocarbides in the HAZ progressively decreases to essentially zero (Fig. 2). On the other hand, as the weld cooling rate is slowed down from 3.7 F/s to only 0.02 F/s, the agglomeration of borocarbide particles becomes significant. This agglomeration is quite similar, in appearance, to the overaging of second phase precipitates in age hardening alloys. Even though the total number of intergranular borocarbides in the HAZ decreases with extremely slow weld cooling rates, the average particle size coarsens. Consequently for slow cooling rates, few active nuclei at grain boundaries are capable of precipitating borocarbides but much diffusion time is available for migration of boron atoms resulting in a few coarse intergranular borocarbides (see Fig. 7b). At weld cooling rates around the optimum of 3.7 F/s, many borocarbide nuclei are precipitated at grain boundaries of austenite and yet there is sufficient diffusion time for the growth of each borocarbide particle, resulting in maximum borocarbide precipitation (see Fig. 5a). Fast weld cooling rates result in numerous potential nucleating sites at austenite grain boundaries but insufficient time for diffusion of boron to develop any significant amount of borocarbide precipitation in the HAZ.

Peak temperatures affect not only the amount of borocarbide precipitating but also where it precipitates in the HAZ. Close to the weld fusion line where the peak temperatures are greater than 2100 F, large amounts of intergranular borocarbides precipitate during weld cooling. This is because the solid solubility of boron in 10B20 steel increases with increasing temperature in the austenite field so more segregation of boron to grain boundaries is permitted at the high temperatures than at the lower austenitizing temperatures (i.e., below about 1800 F).

Thus, austenite grain boundaries in the HAZ which experience high peak temperatures are capable of being saturated with more boron than grain boundaries which are further away from the weld and exposed to lower peak temperatures. As a result, during weld cooling, the high peak temperature boundaries are supersaturated with boron and quickly precipitate intergranular borocarbides while the lower peak temperature boundaries contain too little boron for supersaturation so no borocarbides occur, as was evident in Fig. 8.

Postweld normalizing or annealing at low austenitizing temperatures (between 1580 and 1700 F) is the most effective method to totally eliminate previously formed intergranular borocarbides in the HAZ of 10B20 boron steel. Although postweld heat treatment in this temperature range causes borocarbides to slowly dissolve into the austenite matrix, the rapid dissolution of borocarbides, which was experimently observed, is augmented by the nucleation of new austenite grains at the carbide-ferrite interfaces in pearlite or bainite. Here, the borocarbides at annealing or normalizing temperatures find themselves no longer located at grain boundaries but are now positioned within grains of austenite. This greatly increases the surface energy of each borocarbide particle and promotes a more rapid dissolution of borocarbides.

As the particles dissolve, intersitial boron atoms are free to migrate in

search of defects and grain boundaries around which to form an atmosphere. However, at such low austenitizing temperatures, insufficient boron can accumulate at grain boundaries to produce renewed borocarbide precipitation upon subsequent cooling below the proeutectoid ferrite and eutectoid transformations. Consequently, elimination of previously formed intergranular borocarbides in the HAZ can be rapidly and easily accomplished by either annealing or normalizing operations.

Conclusions

The formation of intergranular borocarbides in the HAZ of SMA and GMA welds deposited on 10B20 boron steel can be characterized by the following:

1. The amount of borocarbides, which form at prior austenite grain boundaries in the HAZ during weld cooling, is dependent upon the weld cooling rate according to the relationship:

$$B = -0.74 \left(\log \frac{dT}{dt} + 2\right)^3 + 2.85 \left(\log \frac{dT}{dt} + 2\right)^2 + 3.74$$

for weld cooling rates between 0.02 F/s to 140 F/s. There is an optimum weld cooling rate of 3.7 F/s which produces the maximum amount of borocarbide precipitation. Above 3.7 F/s, the amount of precipitation decreases until no borocarbides are able to form at cooling rates greater than 140 F/s. From 3.7 F/s down to 0.02 F/s, the amount of borocarbides gradually decreases while the average borocarbide particle size becomes coarser.

2. High peak temperatures (above 2100 F) in the HAZ result in substantial intergranular borocarbide precipitation upon cooling while low peak temperatures (below 1800 F) result in negligible precipitation. However, this amount of borocarbides forming at the high peak temperatures is still dependent upon the weld cooling rate in accordance with the above equation.

3. The welding process used (SMAW and GMAW) is not a factor in the formation of borocarbides.

4. Postweld annealing or normalizing between 1580 F and 1700 F can completely eliminate previously formed intergranular borocarbides in the HAZ.

Thus, for typical SMA and GMA weld cooling rates commonly encountered in commercial welding practice, it is highly probable that the HAZ of 10B20 steel and undoubtedly other boron steels will contain substantial amounts of intergranular borocarbide precipitation. This may possibly be harmful in applications where hardenability and notched toughness are critical.

References

1. Melloy, G. F., Slimmon, P. R. and Podgursky, P. P., "Optimizing the Boron Effect." *Metallurgical Transactions*, Vol. 4, 1973, pp. 2279 to 2289.
2. Grange, R. A. and Mitchell, J. B., "On the Hardenability Effect of Boron in Steel," *Transactions ASM*, Vol. 53, 1961, pp. 157 to 185.
3. Devletian, J. H. and Heine, R. W., "The Effect of Boron Content on Carbon Steel Welds," *Welding Journal*, Vol. 54 (2), Feb. 1975, Research Suppl., pp. 45-s to 53-s.
4. Hughes, J. D. H. and Rogers, G. T., "High-Resolution Autoradiography of Trace Boron in Metals and Solids," *Journal of Institute of Metals*, Vol. 95, 1967, pp. 299 to 301.
5. Adams, Jr., C. M., "Cooling Rates and Peak Temperatures in Fusion Welding," *Welding Journal*, Vol. 37 (5), May 1958, Research Suppl., pp. 210-s to 215-s.
6. Signes, E. G., "A Simplified Method for Calculating Cooling Rates in Mild and Low Alloy Steel Weld Metals," *Welding Journal*, Vol. 51 (10), Oct. 1972, Research Suppl., pp. 473-s to 484-s.
7. Dorschu, K. E., "Control of Cooling Rates in Steel Weld Metal," *Welding Journal*, Vol. 47 (2), Feb. 1968, Research Suppl., pp. 49-s to 62-s.